Electronic properties of Fe_n on Pd(111): From single adatoms to islands

M. Wasniowska,* P. A. Ignatiev, V. S. Stepanyuk, and J. Kirschner
Max-Planck-Institut für Mikrostrukturphysik, Weinberg 2, D-06120 Halle, Germany
(Received 27 September 2008; revised manuscript received 12 March 2009; published 8 April 2009)

The electronic structure of small Fe nanoclusters was investigated by means of scanning tunneling microscopy/spectroscopy and *ab initio* calculations. Unoccupied electronic states of Fe were found for all the examined nanostructures. *Ab initio* calculations clarify that STS actually probed *s-p* electrons resonantly scattered at d_{z^2} states of Fe nanostructures.

DOI: 10.1103/PhysRevB.79.165411 PACS number(s): 73.20.At, 68.37.Ef, 71.15.Mb

Undoubted advances in modern science and technology tend to extreme miniaturization of elements of magnetoelectronic devices down to an atomic scale. Electronic and magnetic properties of such systems are governed by quantum effects and depend on a great extent upon the exact structure and atomic species involved. The development of the low-temperature scanning tunneling microscopy/spectroscopy (LT STM/STS) techniques has induced intensive studies on nanoscale and subnanoscale atomic structures. STM provides a powerful tool for atomic manipulations: dimers, small clusters,[1] branched wires,[2] linear chains,[3] and large atomic corrals[4] can be assembled by means of the STM. At the same time, STS maps electronic and magnetic properties in the atomic resolution, thus allowing detailed studies of adatoms and small clusters adsorbed on metal or semiconductor surfaces.

The first STS studies of single Fe adatoms adsorbed on metallic Pt(111) substrate were performed by Crommie *et al.*[5] The spectra they acquired above Fe adatoms exhibited a resonance at +0.5 eV relative to the Fermi energy (E_F). This feature had a width of approximately 0.6 eV and disappeared after a tip was moved away from the Fe adatom. Room-temperature STS investigations of Fe adatoms on W(110) by Bode *et al.*[6] revealed a similar empty-state peak at 0.5 eV above E_F. The spectra of Fe adsorbates appeared to be independent from the chosen substrate and therefore they were suggested to be quite a general fingerprint of Fe species.

The origin of the resonance at +0.5 eV has been discussed in the literature since the invention. Crommie *et al.*[5] claimed that the resonance centered at +0.5 eV originated from the Fe *s* orbital. This conclusion was based on the work by Lang,[7] who considered a "prototype" transition-metal adatom (Mo) and found that it induced two resonances: a narrow *d*-resonance ($\sim$1 eV wide) slightly below E_F and a broader *s* resonance ($\sim$2 eV wide) centered approximately 1 eV above E_F. Note that the STS feature was observed by Crommie *et al.*[5] exactly in between these two energies. Moreover, these results are supported by the paper by Lee *et al.*,[8] who showed that the STS performed on Co, Fe, and Mn adatoms was insensitive to the spatially localized *d* states. On the other hand, STS on Co on Pt(111) revealed distinct peak features slightly below E_F,[9,10] and the reasoning of Lang unambiguously links them to *d* states of Co. Some additional important information can be achieved from *ab initio* calculations. Co and Fe adatoms on metal surfaces are generally characterized by the minority *d* states situated near E_F.[8,11] In particular, on Cu(111) substrate *d* states of Co and Fe adatoms fall at 0.0 and +0.2 eV, respectively,[11] on Pt(111) at $\sim$0.0 and $\sim$0.35 eV,[12] on Ir(111) at 0.0 and $\sim$+0.5 eV,[12] on Au(111) at 0.0 (Ref. 13) and +0.3 eV,[14] on NiAl(110) at 0.0 and $\sim$+0.5 eV. Lounis *et al.*[11] recently demonstrated that reduced symmetry for adatom on a surface allows resonant scattering of *s* and p_z states at the so-called d_{z^2}-virtual bound states of adatoms,[15,16] so the intensity of *s-p* electrons above the adatom increases. It was claimed that such *s*-p_z resonances (but not d_{z^2} states directly) could be detected by STS.

In this combined experimental and theoretical work we study the electronic structure of small Fe nanoclusters on Pd(111) substrate. The Fe "fingerprint" resonance found by STS at $\approx$+0.5 eV for Fe is attributed by the theory to the resonant scattering of *s-p* electrons at *d*-virtual bound state of Fe.[11] According to our experimental and theoretical results, the exact position of this resonance depends on the absorption site of the Fe adatom. Strong variations in the positions of Fe d_{z^2} states are revealed in small Fe nanoclusters: Fe fingerprint STS resonance splits and then gradually transforms into spectrum of Fe monolayer with the increase in the size of Fe_n nanoclusters. These observations are supported by *ab initio* calculations.

All experiments have been carried out in an ultrahigh vacuum (UHV) system consisting of a preparation-analysis chamber for sample's treatment and for sample's surface characterization by means of low-energy electron diffraction (LEED) and Auger electron spectroscopy (AES). The STM measurements were performed at 5 K with Omicron STM located in separate STM chamber. The base pressure in our measurement system is in the low 10^{-11} mbar range. The Pd(111) single crystal was cleaned by Ar^+-ion sputtering using a sputter gun at 300 K and subsequent annealing for 10 min at T=820 K. The impurity concentration (e.g., C, O, S) is below the AES sensitivity limit of the spectrometer and a sharp $p(1\times1)$ LEED pattern was observed. Fe deposition was performed at $\approx$6 K with deposition rates of 0.02 monolayer (ML)/min. Iron dimers, trimers, and clusters were assembled by means of atom manipulation by the STM tip at tunneling resistance of $\sim$1 MΩ at 5 K.[17] All STS measurements were performed at $\sim$5 K. We used several tungsten tips for recording spectra for clusters electronic structure. It should be noted that STS spectra for single adatoms were sometimes tip dependent for negative sample bias. All dI/dU spectra were measured by adding a modulation voltage U_{mod}=5 $\mathrm{mV_{rms}}$ and the frequency 17.1 kHz to the applied

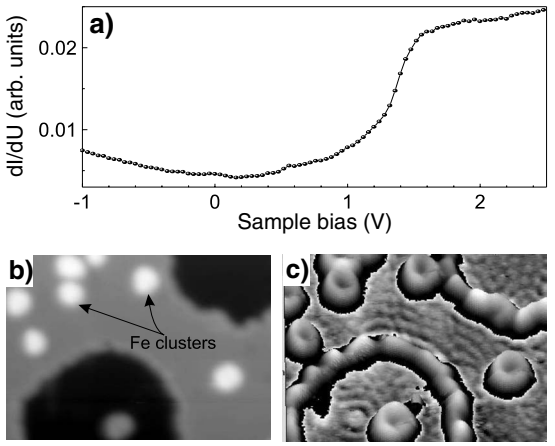

FIG. 1. (a) dI/dU spectrum of defect and impurity free area of Pd(111) acquired at $T=5$ K. Distinctive steplike feature at ~ 1.2 eV is the onset of Pd(111) surface state. The tunneling gap was set at $I=49$ nA and $U=-3$ V. (b) 11.3×9.02 nm^2 topographic image of Pd(111) surface with two vacancy islands (black areas) and Fe clusters (bright spots) ($I=9.0$ nA, $U=2.52$ V). (c) dI/dU map of the same sample area as in (b) recorded at $U=2.52$ V. Standing-wave patterns of Pd(111) surface state are clearly visible.

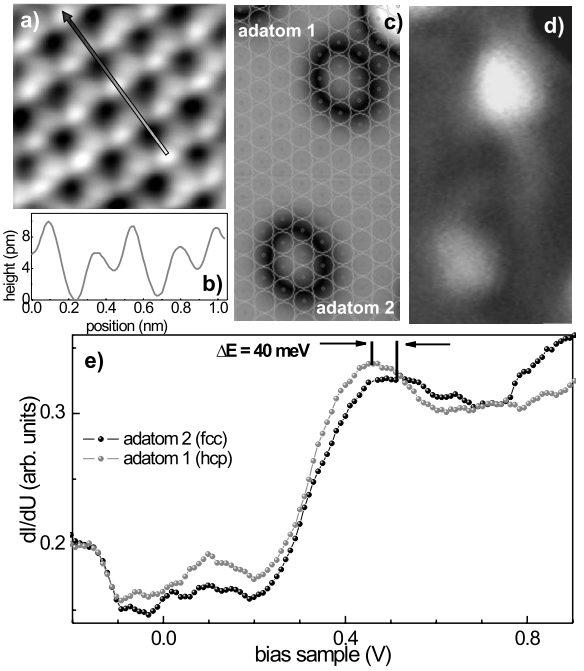

FIG. 2. (a) 1.2×1.2 nm^2 STM image of Pd(111) surface in atomic resolution revealing different hollow sites image of Pd(111) at $T=5$ K [$U=-59.1$ mV and $I=15.6$ nA]. (b) The line profile recorded at the line drawn in (a). (c) 1.7×3.3 nm^2 constant current image of a part of Pd(111) substrate with two Fe adatoms. Stabilization parameters are $I=4.0$ nA and $U=+0.18$ eV. (d) dI/dU map of the same part of the surface simultaneously acquired at $U=+0.18$ eV. Two Fe adatoms exhibit distinct contrast. (e) STS measured on these two Fe adatoms at $I=4.0$ nA and $U=-1$ V.

sample bias U and recording the dI/dU signal by a lock-in technique to obtain information on the local density of states (LDOS) of iron on Pd(111).

Previous inverse photoemission,[18] two photon photoemission studies,[19] as well as theory calculations[20] revealed the existence of the unoccupied Shockley-type surface state on Pd(111) surface. Such a surface state is localized in the vacuum above surface atoms and can be treated as a quasi-two-dimensional (2D) electron gas with a parabolic dispersion law.[21] The band bottom of the unoccupied Pd(111) Shockley surface state was found at ~ 1.3 eV (Ref. 19); its effective electron mass is equal to $0.3m_e$. Theoretical investigations of Heinrichsmeier *et al.*[20] performed by means of nonlocal density-functional theory (DFT) yielded a lower value of surface-state band bottom (0.9 eV) and effective electron mass ($0.22m_e$). STS is able to detect the surface state since it decays to the vacuum slower than Bloch states of a crystal.[5,22] Typical spectra acquired on Pd(111) substrate is demonstrated in Fig. 1(a). A very distinctive steplike feature at ~ 1.2 eV is the onset of the Pd(111) surface state. Scattering of surface-state electrons at surface defects results in the formation of standing-wave patterns.[23,24] Figures 1(b) and 1(c) demonstrate a topographical image of a part of Pd(111) surface with two vacancy islands and a number of Fe nanoclusters and the corresponding differential conductance map with standing-wave patterns of surface-state electrons, respectively.

The electronic structure of a single Fe adatom plays a key role in development of electronic states of larger Fe clusters. This is the reason why we want to pay special attention to the STS on Fe adatoms. Bulk Pd has the face-centered-cubic (fcc) crystal structure, so a Pd(111) surface provides two different kinds of two threefold symmetry hollow sites: fcc and hexagonal-close-packed (hcp). Atoms occupying fcc sites continue normal fcc stacking order of the substrate, while adatoms in hcp sites fault it. Figure 2(a) shows a topographical image of the Pd(111) surface in atomic resolution. Three different kinds of sites are clearly visible although we cannot unambiguously identify them. The apparent height between these sites is illustrated in line profile in Fig. 2(b). In-plane distance between nearest sites of the same kind 0.271 nm corresponds to the fcc lattice constant equal to 0.389 nm, which is in a very good agreement with available experimental data.

Figure 2(c) demonstrates a constant current image of Pd(111) surface with two Fe adatoms stuck in fcc and hcp hollow sites. Substrate Pd atoms are sketched upon the STM image with gray circles. Two bright spots correspond to Fe adatoms occupying fcc and hcp hollow sites. However, it is not entirely clear from this topography map which kind of site each adatom occupies; the spectroscopical contrast between these atoms demonstrated in Fig. 2(d) is evident. Detailed STS studies of Fe adatoms revealed that both for fcc and hcp sites spectra of adatoms were characterized by a broaden peak at approximately +0.5 eV with respect to the Fermi energy, similar to the results by Crommie *et al.*[5] for Fe atoms on Pt(111). In our case, however, the exact energy position of this resonance depends on the adatom stacking. Fe adatom in one of the positions exhibit a peak shifted by 40 meV to higher energies relative to the spectrum of adatom in the second position, as is shown in Fig. 2(e). Another, less pronounced dI/dU feature is a resonance at +0.1 eV. It lies

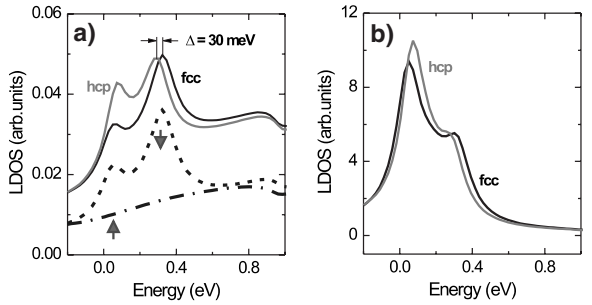

FIG. 3. (a) The total LDOS's calculated at 2.2 Å above the Fe adatom in fcc and hcp binding sites are plotted with solid black and gray curves, respectively. Black dashed and dash-dotted curves demonstrate the minority and majority LDOSs above Fe adatom in fcc hollow site. The peak at +0.35 eV is formed by minority states. (b) The minority spin-polarized *d*-partial LDOS calculated at Fe adatoms in fcc (black) and hcp (gray) hollow sites.

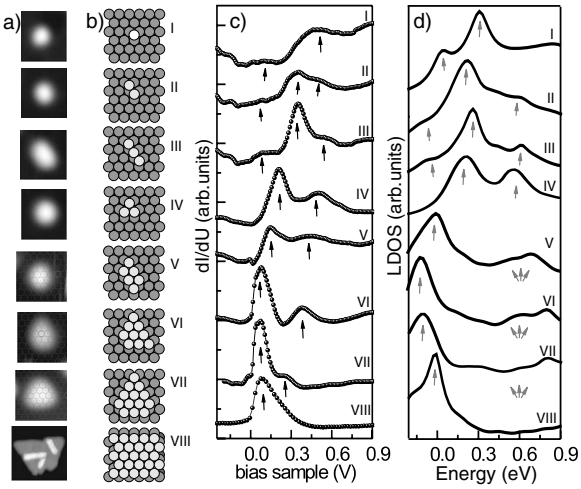

FIG. 4. (a) Constant current images of Fe_n nanoclusters being investigated. Image sizes: 2.18×2.06 nm^2 for I-IV and 2.28×2.24 nm^2 for V-VII. VIII–a Fe island grown at 210 K. Gray area is one layer high part of the island, bright protrusions are the second layer. The spectrum was measured on the gray part. The scale size is 23.5×27 nm^2. (b) Corresponding atomistic structures. (c) STS spectra acquired above all the structures shown in (a) and (b). (d) LDOS calculated in the vacuum 2.4 Å above the nanostructures.

at the same energy for both stackings but its intensity is considerably higher for Fe adatoms occupying the hollow sites where the energy of the main peak at $\simeq+0.5$ eV is lower [Fig. 2(e)].

To demonstrate the origin of the resonance observed in STS experiments we perform *ab initio* calculations by means of the Korringa-Kohn-Rostoker (KKR) Green's-function method.[25–27] This method is the most effective tool for *ab initio* description of impurities embedded into an infinite bulk or placed on an infinite surface. The KKR Green's-function method is the implementation of the DFT and exploits the multiple-scattering formalism to solve the Kohn-Sham equations formulated in the DFT. Mathematically, the KKR method rests on two facts: the local electronic density is completely described by the Green's function of a system; the Green's function of a perturbed system can be expressed from the Green's function of the reference system by means of the Dyson equation. Such a construction makes it possible to express any perturbed system in terms of the reference one. More precisely, a bulk crystal is treated as a periodical in three-dimension (3D) perturbation of free space. The Dyson equation in this case is formulated in the reciprocal space. A surface, accordingly, can be considered either as a 2D perturbation of an infinite bulk crystal or as a 2D slab, which perturbs free space. Finally, a cluster on the surface is a real-space perturbation of an infinite surface and, therefore, can be also studied by means of the KKR. The form and the size of a region perturbed by the cluster at the surface are not restricted to some method-related parameters, such as supercell sizes in plane-wave codes, so systems spread over several nanometers can be studied by the KKR.[24,28,29] Atomic relaxations can be included in the KKR method. However, in our case the main goal of the paper is to reveal tendencies in the evolution of electronic states going from a single adatom to monolayers, therefore we neglect atomic relaxation.

To understand the STS data, we calculate LDOS in the vacuum sphere at 2.2 Å above Fe adatom. Such LDOSs for adatoms placed in fcc and hcp hollow sites are demonstrated in Fig. 3(a). Electronic states above magnetic Fe become spin polarized in a good agreement with the previous calculations on similar systems.[8,11] Two pronounced peaks comprised of *s* and *p* electrons at +0.35 and +0.1 eV are of the minority character. According to our results, stacking of adatom affects the position of the main peak. It is found to be at +0.31 and +0.28 eV for Fe in fcc and hcp hollow sites, respectively. To reveal the origin of these peaks we analyzed the density of states calculated at Fe adatom [Fig. 3(b)]. Two *d* peaks of minority character were found at +0.05 and +0.31 eV for Fe in fcc hollow site and at 0.08 and 0.28 eV for Fe in hcp hollow site. Pronounced peaks observed in the LDOS calculated in vacuum above Fe adatom occur due to resonant scattering of conduction s-p_z electrons at the minority d_{z^2} states of Fe atoms. Splitting of *d* states of Fe adatom is caused by the interaction of Fe adatom with the substrate. Similar splittings were reported for the LDOSs of Fe adatom on Au(111).[14] They were also evidenced for Fe on Pt(111) and Ir(111) substrates.[12]

Now, we turn to our results on small Fe nanoclusters. They were constructed in the UHV chamber in the following way. At first a few percent of ML of Fe was deposited on the Pd(111) surface at 6 K. Thermally activated adatom diffusion, according to our experimental observations, is impossible at a such low temperature. Single adatoms deposited on the surface were used to assemble Fe clusters of desired sizes by means of STM atomic manipulation.[17] The topographies of adatoms, dimers, timers, and small clusters, as well as the number of Fe atoms involved in construction are demonstrated in Fig. 4(a). All the presented structures are visible as bumps with different shapes and sizes. Atomistic models of observed Fe_n nanoclusters are presented in Fig. 4(b). These structures were used in calculations. The shapes of nanoclusters and the number of Fe atoms involved in construction were deduced from the STM images acquired before and after STM manipulations. All the observed Fe clusters are stable and their structure does not change during the STM/

STS measurements. *Ab initio* estimations of binding energies confirm the stability of investigated Fe_n nanoclusters.

Spectra obtained on Fe_n clusters are presented in Fig. 4(c). The electronic structure changes with the number of Fe atoms in clusters. The simplest description of the phenomenon can be obtained, for instance, by means of a tight-binding model including nearest-neighbor interactions only. In this case a dimer is associated with a duplet, a trimer—with a triplet, etc. However, one should keep in mind that Fe nanostructures are supported by the substrate and interaction with the substrate atoms should also be taken into account. Such interactions can split and broaden Fe states. Indeed, as we have just demonstrated in Fig. 3, Fe monomer stuck in fcc hollow site demonstrates the pronounced broad resonance at +0.45 eV and a smaller one at +0.1 eV. The second important point is that *d*-like orbitals are localized and STS is sensitive to s-p_z resonances arising due to scattering of *s* and *p* electrons at d_{z^2} states of nanostructures.[11] In other words, the STS does not probe all the split peaks but only those which have d_{z^2} symmetry.

Adding the second Fe atom to the Fe monomer introduces a possibility of Fe-Fe bonding inside the dimer. This should result in the splitting of *d* states into a duplet. At the same time every Fe atom in the dimer interacts with a substrate Pd atoms. This kind of the interaction can induce an additional states in the LDOS of Fe dimer at the Fermi energy like it happens for the monomer. Resulting LDOS calculated at 2.2 Å above the center of the dimer is shown in Fig. 4(d). It exhibits two broad peaks at +0.2 and +0.6 eV and a broad shoulder at the Fermi energy (all the features are marked by small vertical arrows). The gap between peaks is almost closed and this energy window can contain unresolved spectral features. Experimental observation demonstrated in Fig. 4(c) provides a very similar spectrum of the Fe dimer: two merged peaks at +0.3 and +0.5 eV and a broad shoulder at the Fermi energy. It should be noted, that the sign of the exchange interaction in Fe dimer on Pd(111) can be estimated by means of STS results.[8] In ferromagnetic dimers, in contrast to antiferromagnetic ones, the *d*-derived peak should be split in a duplet.[30] Thus, splitting of the resonance revealed in the experiment indicates the ferromagnetic coupling between Fe atoms in the compact dimer.[30] *Ab initio* calculations confirm this prediction: the ferromagnetic alignment of Fe atoms in the dimer is by 0.243 eV more preferable than the antiferromagnetic one.

At first glance, the STS and LDOS obtained above the center of the linear trimer [Figs. 4(c) and 4(d)] resemble much of the dimer spectrum. But two major differences should be emphasized: a broad peak resurrects in the STS from the shoulder at the Fermi energy and the peak at +0.3 becomes very distinct. The theoretical calculations reproduce these three peaks.

Let us proceed now from linear structures to compact ones. Special threefold symmetry of fcc (111) surfaces implies two possible trimer structures: the first compact trimer has the substrate atom underneath its center and the second has an hcp hollow site in the center. They can be represented on the (111) surface as triangles pointing in the opposite directions. It is clear that substrate-induced splitting of *d* states in the Fe trimer should be different for different arrangements of substrate atoms, so at first, we determine which kind of trimers is energetically more stable. Our *ab initio* calculations demonstrated that the binding energy of the compact Fe trimer with a substrate atom underneath is by 1.38 eV lower than that of another trimer structure.

The STS on the center of the compact trimer shown in Fig. 4(c) is quite different from that acquired above the linear trimer. The main differences are that the distinct peak is situated much closer to the Fermi energy, and there is no more special feature at the Fermi energy. The second peak is situated at +0.5 eV. *Ab initio* results reflect these changes: the LDOS calculated above the center of the compact trimer exhibits two distinct peaks at +0.15 and +0.5 eV [Fig. 4(d)]. These two pronounced peaks preserve in spectra of larger nanostructures. One can see them in the STS measured on centers of Fe_6, Fe_9, Fe_{13}, and Fe ML [Fig. 4(c)]. *Ab initio* LDOSs calculated at 2.2 Å above the centers of these nanostructures reproduce the behavior of the main peak at a lower energy. The second peak at higher energies is, however, represented in *ab initio* results by a complicated features consisting of several broad peaks marked by triple arrows in Fig. 4(d). Similarity of the spectra of all compact Fe nanostructures can be explained by the same splitting of the Fe *d* states so that the energies of the Fe d_{z^2} states are almost the same. The same splitting, in turn, is determined by the same local arrangement of Fe and Pd atoms: all the compact structures are built of compact trimers.

In summary, we have presented the investigation of the Fe clusters on the Pd(111) substrate. We have focused on the spectroscopy of the Fe nanostructures of various sizes from single adatoms to large Fe islands. Small Fe clusters were assembled by means of the STM manipulation. Our STS studies on Fe adatoms revealed a pronounced unoccupied resonance at +0.45 eV above the Fermi energy, which was attributed by *ab initio* calculations to the *s*-*p* states resonantly scattered at the minority d_{z^2} states of the Fe. The exact energy of this resonance was found to depend on the kind of the absorption site of the Fe adatom. The STS study of the larger Fe nanostructures demonstrated splittings and shifts of this resonance caused by the structure-promoted changes in *d* states of the Fe. Analysis of the STS data revealed a gradual transition of the spectrum of the compact Fe trimer to the spectrum of the Fe ML with increasing the cluster size.

This work was supported by the Deutsche Forschungsgemeinschaft under Grants No. SPP 1153 and No. 1165.

*Present address: Max-Planck-Institut für Festkörperforschung, Heisenbergstr. 1, D-70569 Stuttgart, Germany.

[1] J. Lagoute, X. Liu, and S. Fölsch, Phys. Rev. Lett. **95**, 136801 (2005).

[2] J. Lagoute, X. Liu, and S. Fölsch, Phys. Rev. B **74**, 125410 (2006).

[3] J. Lagoute, C. Nacci, and S. Fölsch, Phys. Rev. Lett. **98**, 146804 (2007).

[4] E. J. Heller, M. F. Crommie, C. P. Lutz, and D. M. Eigler, Nature (London) **369**, 464 (1994).

[5] M. F. Crommie, C. P. Lutz, and D. M. Eigler, Phys. Rev. B **48**, 2851 (1993).

[6] M. Bode and R. Wiesendanger, Z. Phys. B: Condens. Matter **99**, 143 (1996).

[7] N. D. Lang, Phys. Rev. Lett. **58**, 45 (1987).

[8] H. J. Lee, W. Ho, and M. Persson, Phys. Rev. Lett. **92**, 186802 (2004).

[9] Y. Yayon, X. Lu, and M. F. Crommie, Phys. Rev. B **73**, 155401 (2006).

[10] F. Meier, L. Zhou, J. Wiebe, and R. Wiesendanger, Science **320**, 82 (2008).

[11] S. Lounis, P. Mavropoulos, P. H. Dederichs, and S. Blügel, Phys. Rev. B **73**, 195421 (2006).

[12] C. Etz, J. Zabloudil, P. Weinberger, and E. Y. Vedmedenko, Phys. Rev. B **77**, 184425 (2008).

[13] O. Šipr, S. Bornemann, J. Minár, S. Polesya, V. Popescu, A. Šimunek, and H. Ebert, J. Phys.: Condens. Matter **19**, 096203 (2007).

[14] M. Weissmann and A. M. Llois, Phys. Rev. B **63**, 113402 (2001).

[15] J. Friedel, Nuovo Cimento **7**, 287 (1958).

[16] G. Gruner and A. Zawadowski, Rep. Prog. Phys. **37**, 1497 (1974).

[17] D. M. Eigler and E. K. Schweizer, Nature (London) **344**, 524 (1990).

[18] S. L. Hulbert, P. D. Johnson, and M. Weinert, Phys. Rev. B **34**, 3670 (1986).

[19] A. Schäfer, I. L. Shumay, M. Wiets, M. Weinelt, Th. Fauster, E. V. Chulkov, V. M. Silkin, and P. M. Echenique, Phys. Rev. B **61**, 13159 (2000).

[20] M. Heinrichsmeier, A. Fleszar, W. Hanke, and A. G. Eguiluz, Phys. Rev. B **57**, 14974 (1998).

[21] N. Memmel, Surf. Sci. Rep. **32**, 91 (1998).

[22] L. C. Davis, M. P. Everson, R. C. Jaklevic, and W. Shen, Phys. Rev. B **43**, 3821 (1991).

[23] M. F. Crommie, C. P. Lutz, and D. M. Eigler, Nature (London) **363**, 524 (1993).

[24] V. S. Stepanyuk, L. Niebergall, W. Hergert, and P. Bruno, Phys. Rev. Lett. **94**, 187201 (2005).

[25] K. Wildberger, V. S. Stepanyuk, P. Lang, R. Zeller, and P. H. Dederichs, Phys. Rev. Lett. **75**, 509 (1995).

[26] R. Zeller, P. H. Dederichs, B. Ujfalussy, L. Szunyogh, and P. Weinberger, Phys. Rev. B **52**, 8807 (1995).

[27] J. Zabloudil, R. Hammerling, L. Szunyogh, and P. Weinberger, *Electron Scattering in Solid Matter* (Springer, New York, 2005).

[28] G. Rodary, D. Sander, H. Liu, H. Zhao, L. Niebergall, V. S. Stepanyuk, P. Bruno, and J. Kirschner, Phys. Rev. B **75**, 233412 (2007).

[29] N. N. Negulyaev, V. S. Stepanyuk, L. Niebergall, P. Bruno, W. Hergert, J. Repp, K.-H. Rieder, and G. Meyer, Phys. Rev. Lett. **101**, 226601 (2008).

[30] A. Oswald, R. Zeller, P. J. Braspenning, and P. H. Dederichs, J. Phys. F: Met. Phys. **15**, 193 (1985).